Immobilization of soybean peroxidase on aminopropyl glass beads: Structural and kinetic studies

Immobilization of Soybean Peroxidase on Aminopropyl Glass Beads: Structural and Kinetic Studies

Tatiana Marchis[a], Giuseppina Cerrato[a,b], Giuliana Magnacca[a,b], Valentina Crocellà[a,b], Enzo Laurenti[a,]*

[a]Università degli Studi di Torino, Department of Chemistry, Via P. Giuria 7, 10125 Torino, Italy

[b]Centre of Excellence NIS, Università degli Studi di Torino, Via Giuria 7, 10125 Torino, Italy

*Corresponding author. Tel: +39 011 670 7951; fax: +39 011 670 7855

E-mail address: enzo.laurenti@unito.it

Abstract

The enzyme Soybean Peroxidase (SBP) is able to catalyse the oxidation of a large number of substrates and is characterized by high resistance to both chemical and thermal denaturation. In this contribution SBP was covalently immobilized on aminopropyl glass beads (APG) in order to obtain a solid biocatalyst, useful either in degradation of pollutants or in specific oxidative reactions. Several samples of immobilized SBP were first synthesized and then characterized by means of some experimental techniques (FT-IR, ESR, and UV-visible spectroscopies, gas-volumetric adsorption of nitrogen at 77K, SEM). Moreover, different kinetic measurements were carried out to determine activity and stability properties of these biocatalysts. Our data indicate that (*i*) the SBP catalytic site was partially modified during the immobilization process, but the enzyme retained about 35% of its specific activity after immobilization, and (*ii*) the biocatalyst exhibits a significant improvement of SBP stability over time, preserving up to 50% of its initial activity after 70 days of storage and 85% when used in ten consecutive reaction cycles.

Keywords

Immobilisation; Immobilised Enzymes; Heterogenous Biocatalysis; Enzyme Activity; Soybean; Peroxidase.

1. Introduction

Enzymes are the catalysts of the living world, but their excellent properties render them also exploitable in many applications that range from industrial catalysis to therapeutics [1]. In recent years, the interest in enzymatic technology increased, because of the growing attention paid to environmental concerns, as well as the need for renewable raw materials. Indeed, many traditional processes have already been replaced by enzyme technology, and its advent has brought benefits like milder conditions of reaction, energy savings, and improvement of health conditions [2].

On the other hand, the issues lying under the practical applicability of many enzymatic processes derive principally from economic problems related to high production costs and technical issues in re-use and storage of enzymes. So, in order to employ biocatalysts in continuous systems, many enzymes were immobilized on different supports by means of several techniques like adsorption, entrapment, or covalent bonding. Immobilized enzymes are generally more stable, easily removable from the reaction bath, and reusable for many reaction cycles, but the choice of the immobilization method is a critical point because the process can drastically modify the properties of the enzyme. In few cases, immobilization results in an increase of catalytic activity [3], but typically a more or less dramatic modification and reduction of the kinetic properties was observed [4-6], so the effect of the immobilization process must be carefully evaluated.

In the present contribution we immobilized commercial samples of Soybean peroxidase (SBP, E.C. 1.11.1.7) on the surface of aminopropyl glass beads (APG) with controlled pore diameter (~550Å). SBP is a class III secretory plant peroxidase [7] implicated in lignification cycle *in vivo* and characterized by a Fe(III)-heme protoporphyrin IX prosthetic group as active site [8]. The catalytic cycle, typical of Fe-heme peroxidases, involves the two-electron reduction of hydrogen peroxide and the one-electron oxidation of two substrate molecules *via* the well characterized intermediates Compound I and

Compound II [9]. Such mechanism allows the oxidation of several inorganic and organic substrates in a broad range of pH values [10]. In addition, SBP exhibits a great stability and resistance to unfolding in the presence of denaturing conditions, such as high temperature, organic solvents, or high ionic strength [11-13]. This features make SBP very interesting for biotechnological applications, such as the biodegradation of wastewaters pollutants like phenol and its halogenated derivatives [6, 14-17] or synthetic dyes [18-19].

Several methods of immobilization have been reported both for SBP and other peroxidases, and different supports have been employed in order to take advantage of their properties in biotechnological applications [5,6, 20-22]. In this work we chose to immobilize SBP through the formation of covalent bonds between the amino groups present on the protein surface, and the aldehyde groups of glutaraldehyde-activated APG in order to obtain a useful and stable biocatalyst.

The resulting samples of immobilized SBP were characterized by means of several experimental techniques (FT-IR, ESR, and UV-visible spectroscopies, gas-volumetric adsorption of N_2 at 77K, SEM) and kinetic measurements in order to establish their activity and stability properties. Our results evidenced how the immobilization process slightly modified the catalytic site of the protein, while SBP still retained a good percentage of its native catalytic activity, and stabilized the enzyme over time.

2. Materials and methods

Aminopropyl glass beads (200-400 mesh particle size, 550 Å average diameter pores, 42.7 $m^2\ g^{-1}$ surface area, $1 \cdot 10^{-2}$ mol g^{-1} amino groups available) and glutaraldehyde (25% water solution) were purchased from Fluka. Soybean peroxidase and hydrogen peroxide (30% water solution) were purchased from Sigma, guaiacol (98%), 3-methyl-2-benzothiazolinone (MBTH), and 3-(dimethylamino)benzoic acid (DMAB) from Aldrich.

2.1 Immobilization procedure

200 μL of glutaraldehyde (25% v/v water solution) were added to 200 mg of APG beads previously suspended in 5 mL of phosphate buffer 0.05 M at pH 7.0, and then the mixture was stirred for 7 hours at room temperature (RT). The excess of glutaraldehyde was removed washing repeatedly the particles with a phosphate buffer solution 0.05 M at pH 7.5. The APG activated beads (APG-G) were suspended in 5 mL of SBP solution at different concentrations ($1.08 \cdot 10^{-5}$-$1.38 \cdot 10^{-4}$ M , 0.4-5.1 mg mL^{-1}), the mixture was left stirring for 17 hours at 3°C, and then the resulting APG-G-SBP beads were filtered and washed many times with the same buffer. The immobilized SBP was left to dry for a few hours in air before storage in dried form at 3°C until use. Reaction times and buffer solutions were chosen in agreement with a procedure previously reported for Horseradish Peroxidase (HRP) [4], whereas enzyme concentration was optimized for SBP as reported in the Results and Discussions section.

The amount of SBP immobilized on APG was calculated as the difference between the initial amount of enzyme and that present in the washing liquid. The concentration of SBP in solution was determined by means of UV-Visible spectroscopy, measuring the absorbance at 403 nm ($\varepsilon_{403\ nm}$ = 96400 M^{-1} cm^{-1} [23]).

2.2 Sample characterization

FT-IR spectroscopy measurements were performed on self supporting pellets (~8 mg cm^{-2}) activated in a quartz cell (equipped with KBr windows) connected to a dynamic vacuum glass line. All samples were activated in vacuo for 2 hours at room temperature and the spectra (4 cm^{-1} resolution) were obtained with an IFS88 Bruker spectrophotometer equipped with MCT cryo-detector.

Nitrogen adsorption-desorption gas-volumetric isotherms were obtained at 77K using a Micromeritics ASAP 2020 automated system. All samples were outgassed in vacuo at

30°C till a very low residual pressure was reached. The surface area was determined using Brunauer-Emmett-Teller (BET) model [24]. The main pore diameter and pore volume of samples were obtained from the Barret-Joyner-Halenda (BJH) method applied to the desorption branch of isotherms [25].

Images of APG-based samples were obtained by means of Scanning Electron Microscopy (SEM, Leica Stereoscope 420). The samples were sputter-coated with gold prior to the observation.

Electron Spin Resonance spectra were recorded at 4 K by an ESP300E Bruker X-band spectrometer equipped with a 4103TM cylindrical cavity and an Oxford Instruments ESR900A cryostat. Commercial SBP was dissolved in phosphate buffer 0.1 M pH 7.0 (final concentration was $3 \cdot 10^{-4}$ M). As reference, 5 mg of APG-G-SBP beads were first analyzed dry and then suspended in 100 μL of the same buffer solution.

2.3 Kinetic measurements

All the kinetic measurements were made in quartz cells with a UNICAM UV300 Thermospectronic double beam UV-visible spectrometer, equipped with a Peltier cell for temperature control.

The evaluation of SBP activity and efficiency after the immobilization procedure was obtained by means of a chromogenic reaction involving guaiacol oxidation to tetraguaiacol, detectable at 470 nm ($\varepsilon_{470\ nm}$ = 26600 $mM^{-1}\ cm^{-1}$ [26]). Preliminary experiments were carried out with SBP in solution, in order to determine the inhibition concentration of H_2O_2 and single out the conditions in which the initial reaction rate depends only on the guaiacol concentration. The optimal concentrations of guaiacol ($1.46 \cdot 10^{-4}$ M) and hydrogen peroxide ($1.64 \cdot 10^{-4}$ M) were determined by preliminary experiments and used to test the activity of the enzyme before and after the immobilization process. In the case of immobilized samples the appropriate concentration of enzyme was

obtained preparing an initial suspension of APG-G-SBP 10 mg mL^{-1} in 0.05 M phosphate buffer pH 7.0, stirring the mixture for 1 hour before measurements and withdrawing the appropriate amount to be added to the reaction batch.

The effect of pH on SBP activity was determined with the same method described above, but using a triple buffer solution 0.05 M acetate, 0.05 M phosphate and 0.05 M borate in order to ensure a good buffering power in the 2-10 pH range. Long term stability of immobilized and soluble SBP, stored at 3°C in dried and hydrated form, was tested periodically by monitoring the initial rate of tetraguaiacol formation.

The efficiency of the solid catalyst was investigated by designing a little sized reactor. A reservoir of stock solution of substrate (DMAB, MBTH or guaiacol) and hydrogen peroxide $2.0 \cdot 10^{-6}$ M in phosphate buffer 0.05 M (pH 7.0) was connected by means of a peristaltic pump to the input of a glass column (30 cm × 2.5 cm ∅) containing 30 mL of APG-G-SBP suspension with a concentration of $1.4 \cdot 10^{-5}$ M SBP. The output of the reactor was then connected to a quartz flow cell in the UV-visible spectrophotometer.

This system was used both in discontinuous and in continuous conditions. In the first case the substrate used was guaiacol and the residence time was 30 min. The APG-G-SBP sample was reused 10 times emptying the column each time from products solution, and replacing it with fresh substrate solution without washing the biocatalyst. In the second case DMAB ($8.5 \cdot 10^{-4}$ M) and MBTH ($3.5 \cdot 10^{-5}$ M) were used as substrates. In the presence of H_2O_2, the enzyme catalyses the oxidative dehydrogenation of MBTH, which in turn reacts with DMAB to give an indamine dye, easily detectable with UV-visible spectroscopy at 590 nm ($\varepsilon_{590\ nm}$ = 47600 $M^{-1}\ cm^{-1}$ [27]), and stable during the measurement time (90 min). The flow of the mixture into the system was adjusted at 2.5 mL min^{-1}.

3. Results and discussions

3.1 Immobilization and characterization

The three-dimensional structure of Soybean Peroxidase (RCSB Protein Data Bank Id. 1FHF [8]) shows the presence on the protein surface of four aminoacids containing free amino groups, useful for the conjugation with free aldehydic groups: three lysines (Lys84, Lys149, and Lys281) and the N-terminal glutamine (Gln1). Therefore soybean peroxidase was immobilized on aminopropyl glass beads previously activated with glutaraldehyde. Both these reactions are expected to proceed through the formation of Schiff bases, as a result of the nucleophilic addition of the aldehyde groups to the amino groups present on APG and on the enzyme surface, respectively.

In order to avoid cross-linking of protein molecules in the presence of free glutaraldehyde, the immobilization process was conducted in two distinct steps and each sample was characterized by means of FT-IR spectroscopy, SEM, and nitrogen adsorption isotherms using BET and BJH methods [24, 25]. The results of these analysis are reported in the following Figures 1-3 and summarized in Table I.

TABLE I

Figure 1 reports the FT-IR spectra obtained after activation *in vacuo* at RT for 1 hr. On the basis of both spectral behaviour and literature data, all the contributions at high frequency (in the 3750-2750 cm^{-1} range) can be ascribed to the stretching vibration of O-H, N-H and C-H species present at the surface of these system [28-31]. These bands are due to either intrinsic or added functionalities present at the sample surface. As for the low frequencies region, the different contributions derives from (*a*) both combination and overtones of Si-O-Si modes (bands at ~ 1990, 1880 and 1650 cm^{-1}) characteristic of the silica network [30], and (*b*) the spectral bending (δ_{NH}) counterpart (band at ~ 1610-1615 cm^{-1}) of the above cited NH surface species [32]. When glutaraldehyde is added to the APG beads, a Schiff base forms with the expected IR bands: a broad envelope centred at ~1660 with a shoulder at ~ 1720 cm^{-1}. Proceeding in the next step of the functionalization by SBP, the

shoulder at 1720 cm^{-1} disappears and the reaction product is characterized by the intense bands at 1660 cm^{-1} due to the presence of the polypeptide chain.

FIGURE 1

Scanning Electron Microscopy (SEM) images (Figure 2) indicate that APG is made up of particles with both irregular shape and size characterized by very smooth surfaces. After the reaction with glutaraldehyde, a decrease of particles size dimensions was observed (see Table I) besides the presence of smaller particles of nanometric size (less than 1 μm) dispersed onto rougher surfaces. Almost no further modifications are induced by protein immobilization.

FIGURE 2

N_2 adsorption at -196°C indicate that all samples are macroporous (a hystheresis loop at relative pressures higher than 0.9 is present in all the isotherms obtained, not shown for the sake of brevity) with a macroporosity formed by void interparticles space given by particles agglomeration. The shape of hystheresis loop can be described as H1 by IUPAC classification, i.e., of a material consisting of agglomerates of approximatively uniform spheres in fairly regular array [33].

The pore size distribution curves, shown in Figure 4, confirm that all systems are macroporous, presenting pores in the range 500-1200 Å of width for all the steps of the immobilization procedure. Small changes in porosity, indicated in Table I, suggesting that protein presence did not affect in significant way the porous framework of APG material, possibly because protein size is negligible compared to APG pore size.

FIGURE 3

The formation of smaller particles, the increase of the surfaces roughness, and the global decrease of the main particles size are reflected by an increase of BET surface areas from 42 to 47 m^2/g. In parallel, the slight increase of macroporosity and the decrease of average pore size diameter might be explained considering two competitive effects: (*i*) addition of

glutaraldehyde to the hydrophilic silica surface may cause an impairment of particles interaction with a subsequent loss of particles agglomeration, increasing the interparticles empty volume (i.e., the total pore volume); (*ii*) functionalization produces smaller aggregates (evidenced by SEM images) which can better pack decreasing the average pores size.

In the final step of immobilization, protein addition is likely to increase the possibility to establish interactions between particles: the total porosity decreases, but steric hindrance inhibits the coalescence of particles resulting in the formation of larger pores.

In order to evaluate the effects of the immobilization process on the SBP catalytic site the APG-G-SBP species was analysed by ESR spectroscopy (Figure 4). In agreement with previous literature data [34], the ESR spectrum of Soybean Peroxidase in solution, reported for comparison, consists of several lines at low field, indicative of the presence of different Fe(III)-heme species, and an additional signal at g = 4.3 due to the presence of Fe(III)-non heme impurity. On the contrary, the APG-G-SBP sample revealed a much simpler spectral pattern, due to the presence of a single axial species with $g_{\perp}$ = 6.04 and $g_{//}$ = 2.0.

Indiani et al. suggested that the ESR spectrum of native SBP results from the presence, at low temperature, of a quantum-mechanical admixture (QS state) of high-spin (HS, S = 5/2) and intermediate-spin (IS, S = 3/2) states, responsible for the rhombic signal (g = 5.93, 5.04, 2.00) and the shoulder feature at g = 6.11. Moreover, a weak low spin (LS, S = 1/2) signal (with g_x = 3.23, g_y =2.07 and g_z not observable in these conditions) is also present and can be ascribed to a *bis*-imidazole species [34].

FIGURE 4

The differences observable in the ESR spectrum of APG-G-SBP are indirect evidence that some conformational changes take place during the immobilization process, the most evident effect being the increased symmetry of the ligands field. The constraints imposed on the protein structure by the formation of covalent bonds with the glass surface seems to:

(*i*) reduce the distortion of the heme plane; (*ii*) slightly modify the disposition of the residues present in the catalytic pocket. The presence of an axial signal with $g_{\perp} \cong 6$ is amenable to the existence of a six-coordinated HS species with a water molecule as a dissociable ligand [9, 35-37]. The complete absence of LS signals is likely to indicate that a *bis*-imidazolate complex cannot be generated in this species, probably because the distance between the distal histidine and the Fe(III) ion is longer than before the immobilization process.

Many attempts of immobilization were made with different amounts of initial protein content: the immobilization percentage and the amount of enzyme loaded on the support were calculated for each test and reported in Figure 5. As expected, the immobilization yield was close to 100% when small amounts of protein were employed, and gradually decreased using initial amounts of SBP larger than 20 mg/g APG. On the contrary, the protein loading increased with the increase of the initial amount of SBP up to a maximum of 29.8 mg SBP/g APG, then it also decreased.

These data are comparable with those obtained for SBP by Gomez et al. [5, 6], and much higher than those previously reported for the immobilization of HRP [4, 5].

FIGURE 5

3.2 Kinetic studies

In order to define the kinetic parameters and the optimal conditions for the activity of the immobilized SBP, kinetic measurements were carried out in many different experimental conditions. First, the activity of SBP towards guaiacol was investigated as a function of enzyme concentration. The initial reaction rate, expressed as μmol of tetraguaiacol produced per min (U), was measured at increasing SBP concentration for many samples of APG-G-SBP with different SBP load, in order to extrapolate the correspondent specific activities (U mg^{-1}) from the slope of each linear regression equation (data not shown). The

enzymatic activity was found to be directly related to the amount of immobilized SBP, and a maximum of 4.61±0.12 U mg^{-1} was obtained for the sample with the higher SBP load. This value corresponds to 35% of the activity measured in the same conditions for the free SBP (13.4 U mg^{-1}).

A partial loss of catalytic activity is usually reported for enzymes subjected to immobilization processes, mainly due to the immobilization of the enzyme in non-achievable positions or to a partial distortion of the active site, as it seems to occur in the present case on the basis of ESR data. However, it is interesting to note that the APG-G-SBP samples mantain a good enzyme activity (as previously reported for a similar system [5, 6]) whereas, in the case of immobilized horseradish peroxidase, the retained activity was only 3% of the initial value [4].

FIGURE 6

The effect of immobilization on the catalytic properties of SBP was also investigated on a wide range of pH values using guaiacol as substrate (Figure 6). The results fitted with a model derived from the Henderson-Hasselbach equation to describe a system undergoing a double ionization process [38, 39], and the pH profile of APG-G-SBP results shifted to highest pH values respect to the free SBP. In fact, the immobilized SBP shows a maximal activity at pH 6.5 and two inflection points at pH 4.7 ± 0.1 and 8.2 ± 0.1, whereas the free SBP has a maximum in correspondence of pH 5.8 and two inflection points at pH 3.8 ± 0.1 and 7.8 ± 0.1. This behaviour was already observed and correlated to the anionic nature of the support since, in the close proximity of the surface, the local pH is slightly lower than that of the bulk phase, and thus leads to the raising of the apparent optimal pH [22, 40].

Both the efficiency and the reusability of the biocatalyst were investigated in a little sized reactor connected with a flux cuvette positioned directly inside the UV-VIS spectrophotometer. In the case of continuous use an alternative substrate to guaiacol was chosen because of instability of tetraguaiacol over the test time. A mixture of

H_2O_2/DMAB/MBTH was introduced in the reactor by means of a peristaltic pump generating a continuous flux of reagents. The reaction was monitored recording for 90 min the absorbance at 590 nm, typical of the indamine dye originated from the coupling of DMAB with the oxidation product of MBTH [27]. The data in Figure 7A clearly shows as the system would be fully operational after a few minutes and retains its catalytic activity for the whole experimental time.

The same reactor was employed in a discontinuous way, performing several cycles of reaction catalyzed by the same sample of APG-G-SBP. In this case a fresh aliquot of guaiacol/H_2O_2 mixture was introduced in the reactor and left to react for 30 min with APG-G-SBP, hence the little sized reactor was emptied, and the amount of tetraguaiacol produced during the reaction was measured. This cycle was repeated ten times and the corresponding results are reported in Figure 7B. After an initial conditioning phase, the activity of APG-G-SBP reached the maximum value during the fourth cycle and then it remained stable at ~85% of maximum activity in the subsequent cycles of reaction. These values are very encouraging, if compared to those previously reported for HRP immobilized on chitosan beads (65% after 6 reaction cycles [22]) or onto APG (50% after 5 cycles [4]).

FIGURE 7

Finally, experimental data on the effect of long term storage at 3°C on the stability of SBP were obtained by measuring the activity of the immobilized SBP and comparing it with a solution of free SBP. The results indicated that APG-G-SBP, both stored in suspension or in dried form, was able to retain its activity for a longer period of time than the soluble one (Figure 8). After the first month of storage, the free enzyme lost about 90% of its specific activity, whereas APG-G-SBP retained more than 50% of initial activity when stored in dried forms, and 30% when stored hydrated at pH 7.0. Looking to the second part of the experiment, it becames evident that the activity of free SBP tends to zero, whereas the

APG-G-SBP samples mantained unaltered their catalytic potential until the end of the period monitored.

FIGURE 8

4. Conclusions

The method employed for SBP immobilization allowed to produce effective biocatalysts with only slight modifications of the catalytic site of SBP, as demonstrated by ESR measurements, and minimal alteration of the APG surface. Moreover, FT-IR spectra and kinetic data confirm the formation of a covalent binding between APG, glutaraldehyde and SBP, and the presence of these constrains stabilize the system against modifications induced by storage, retaining its catalytic properties much longer than free SBP.

To complete the analysis on APG-G-SBP potential, further studies are currently in progress to test the effects of immobilization process on the resistance to heating. Preliminary data suggested an improvement in the resistance of SBP to the denaturation, but these experiments still have to be completed. In any case, the results shown in the present paper for the APG-G-SBP system, in combination with recent literature data reporting the successful applications of SBP in different biotechnological fields [19, 41-42], are encouraging about the possible industrial applications of this system.

References

[1] B.C. Saha, D.B. Jordan, R.J. Bothast,. Enzymes, Industrial (overview), in: S. Moselio (Ed.), Encyclopedia of Microbiology, third ed., Academic Press, Oxford, 2009, pp. 281-294.

[2] A. Schmid, J.S. Dordick, B. Hauer, A. Kiener, M. Wubbolts, B. Witholt, Industrial biocatalysis today and tomorrow, Nature 409 (2001) 258-268.

[3] G. Fernandez-Lorente, M. Terreni, C. Mateo, A. Bastida, R. Fernandez-Lafuente, P. Dalmases, J. Huguet, J.M. Guisan, Modulation of lipase properties in macro-aqueous systems by controlled enzyme immobilization: enantioselective hydrolysis of a chiral ester by immobilized *Pseudomonas* lipase, Enzyme Microb. Technol. 28 (2001) 389-396.

[4] Y.-C. Lai, S.-C. Lin, Application of immobilized horseradish peroxidase for the removal of p-chlorophenol from aqueous solution, Process Biochem. 40 (2005) 1167-1174.

[5] J.L. Gómez, A. Bódalo, E. Gómez, J.Bastida, A.M. Hidalgo, M. Gómez, Immobilization of peroxidases on glass beads: An improved alternative for phenol removal. Enzyme Microb. Technol. 39 (2006) 1016-1022.

[6] M. Gómez, G. Matafonova, J.L. Gómez, V. Batoev, N. Christofi, Comparison of alternative treatments for 4-chlorophenol removal from aqueous solutions: Use of free and immobilized soybean peroxidase and KrCl excilamp,. J. Hazard Mater. 169 (2009) 46-51.

[7] K.G. Welinder, Superfamily of plant, fungal and bacterial peroxidases, Curr. Opin. Struct. Biol. 2 (1992) 388-393.

[8] A. Henriksen, O. Mirza, C. Indiani, K. Teilum, G. Smulevich, K.G. Welinder, M. Gajhede, Structure of soybean seed coat peroxidase: A plant peroxidase with unusual stability and haem-apoprotein interactions, Prot. Sci. 10 (2001) 108-115.

[9] H.B. Dunford, Heme Peroxidases, Wiley-VCH, New York, 1999.

[10] M. Nissum, C.B. Schiødt, K.G. Welinder, Reactions of soybean peroxidase and hydrogen peroxide pH 2.4-12.0, and veratryl alcohol at pH 2.4, Biochim. Biophys. Acta 1545 (2001) 339-348.

[11] J.P. McEldoon, J.S. Dordick, Unusual thermal stability of soybean peroxidase, Biotechnol. Prog. 12 (1996) 555-558.

[12] J.K.A. Kamal, D.V. Behere, Thermal and conformational stability of seed coat soybean peroxidase, Biochemistry 41 (2002) 9034-9042.

[13] B. Boscolo, E. Laurenti, E. Ghibaudi, ESR spectroscopy investigation of the denaturation process of soybean peroxidase induced by guanidine hydrochloride, DMSO or heat,. Protein J. 25 (2006) 379-390.

[14] N. Caza, J.K. Bewtra, N. Biswas, K.E. Taylor, Removal of phenolic compounds from synthetic wastewater using soybean peroxidase, Water Res. 33 (1999) 3012-3018.

[15] A. Bódalo, J.L. Gómez, E. Gómez, J. Bastida, M.F. Máximo, Comparison of commercial peroxidases for removing phenol from water solutions, Chemosphere 63 (2006) 626-632.

[16] A. Bódalo, J. Bastida, M. Máximo, M. Montiel, M. Gómez, M. Murcia, A comparative study of free and immobilized soybean and horseradish peroxidases for 4-chlorophenol removal: protective effects of immobilization, Bioprocess Biosyst. Eng. 31 (2008) 587-593.

[17] A. Steevensz, M.M. Al-Ansari, K.E. Taylor, J.K. Bewtra, N. Biswas, Comparison of soybean peroxidase with laccase in the removal of phenol from synthetic and refinery wastewater samples, J. Chem. Technol. Biotechnol. 84 (2009) 761-769.

[18] K. Knutson, S. Kirzan, A. Ragauskas, Enzymatic biobleaching of two recalcitrant paper dyes with horseradish and soybean peroxidase, Biotechnol. Lett. 27 (2005) 753-758.

[19] T. Marchis, P. Avetta, A. Bianco-Prevot, D. Fabbri, G. Viscardi, E. Laurenti Oxidative degradation of Remazol Turquoise Blue G 133 by soybean peroxidase, J. Inorg. Biochem. 105 (2011) 321-327.

[20] P. Peralta-Zamora, E. Esposito, R. Pelegrini, R. Groto, J. Reyes, N. Durán, Effluent treatment of pulp and paper, and textile industries using immobilised horseradish peroxidase, Environ. Technol. 19 (1998) 55-63.

[21] K.F. Fernandes, C.S. Lima, F.M. Lopes, C.H. Collins, Properties of horseradish peroxidase immobilised onto polyaniline, Process Biochem. 39 (2004) 957-962.

[22] M. Monier, D.M. Ayad, Y. Wei, A.A. Sarhan, Immobilization of horseradish peroxidase on modified chitosan beads, International J. Biol. Macromol. 46 (2010) 324-330.

[23] J.K.A. Kamal, D.V. Behere, Activity, stability and conformational flexibility of seed coat soybean peroxidase, J. Inorg. Biochem. 94 (2003) 236-242.

[24] S. Brunauer, P.H. Emmett, E. Teller, Adsorption of gases in multimolecular layers, J. Am. Chem. Soc. 60 (1938) 309-319.

[25] E.P. Barrett, L.G. Joyner, P.P. Halenda, The determination of pore volume and area distributions in porous substances. I. Computations from nitrogen isotherms, J. Am. Chem. Soc. 73 (1951) 373-380.

[26] K.K. Mäkinen, J. Tenovuo, Observations on the use of guaiacol and 2,2'-azino-di(3-ethylbenzthiazoline-6-sulfonic acid) as peroxidase substrates, Anal. Biochem. 126 (1982) 100-108.

[27] T.T. Ngo, H.M. Lenhoff, A sensitive and versatile chromogenic assay for peroxidase and peroxidase-coupled reactions, Anal. Biochem. 105 (1980) 389-397.

[28] L.H. Little, Infrared spectra of adsorbed species, Academic Press, London, 1966.

[29] A.P. Legrand, The surface properties of silicas, J Wiley & Sons, Chichester, 1998.

[30] L. Contessotto, E. Ghedini, F. Pinna, M. Signoretto, G. Cerrato, V. Crocellà, Hybrid organic–inorganic silica gel carriers with controlled drug-delivery properties, Chem. Eur. J. 15 (2009) 12043-12049.

[31] E. Ghedini, M. Signoretto, F. Pinna, V. Crocellà, L. Bertinetti, G. Cerrato, Controlled release of metoprolol tartrate from nanoporous silica matrices, Microporous Mesoporous Mat. 132 (2010) 258-267.

[32] G Herzberg, Molecular Spectra and Molecular Structure. II. Infrared and Raman spectra of polyatomic molecules, Van Nostrand, New York, 1945.

[33] K.S.W. Sing, Reporting physisorption data for gas/solid systems with special reference to the determination of surface area and porosity (Recommendations 1984), Pure Appl. Chem. 57 (1985) 603-619.

[34] C. Indiani, A. Feis, B.D. Howes, M.P. Marzocchi, G. Smulevich, Effect of low temperature on soybean peroxidase: spectroscopic characterization of the quantum-mechanically admixed spin state, J, Inorg, Biochem, 79 (2000) 269-274.

[35] G. Palmer, Electron paramagnetic resonance of hemoproteins, in A.B.P. Lever, H.B. Gray (Eds.), Iron Porphyrins, Part 2, Addison-Wesley Publishing Company, Reading, 1983, pp. 45-88.

[36] M. Ikeda-Saito, H. Hori, L.A. Andersson, R.C. Prince, I.J. Pickering, G.N. George, C.R. Sanders, R.S. Lutz, E.J. McKelvey, R. Mattera, Coordination structure of the ferric heme iron in engineered distal histidine myoglobin mutants, J. Biol. Chem. 267 (1992) 22843-22852.

[37] E. Laurenti, G. Suriano, E.M. Ghibaudi, R.P. Ferrari, Ionic strength and pH effect on the Fe(III)-imidazolate bond in the heme pocket of horseradish peroxidase: an EPR and UV-visible combined approach, J. Inorg. Biochem. 81 (2000) 259-266.

[38] P.K. Patel, M.S. Mondal, S. Modi, D.V. Behere, Kinetic studies on the oxidation of phenols by the horseradish peroxidase compound II, Biochim. Biophys. Acta 1339 (1997) 79-87.

[39] E. Laurenti, E. Ghibaudi, S. Ardissone, R.P. Ferrari, Oxidation of 2,4-dichlorophenol catalyzed by horseradish peroxidase: characterization of the reaction mechanism by UV-visible spectroscopy and mass spectrometry, J. Inorg. Biochem. 95 (2003) 171-176.

[40] M. Chaplin, C. Bucke, Enzyme technology, University Press, Cambridge, 1990.

[41] M.M. Vdovenko, A.V. Zubkov, G.I. Kuznetsova, L. Della Ciana, N.S. Kuzmina, I.Y. Sakharov, Development of ultra-sensitive soybean peroxidase-based CL-ELISA for the determination of human thyroglobulin, J. Immunol. Methods 362 (2010) 127-130

[42] A. Tewari, A. Kokil, S. Ravichandran, S. Nagarajan, R. Bouldin, L.A. Samuelson, R. Nagarajan, J. Kumar, Soybean peroxidase catalyzed enzymatic synthesis of pyrrole/EDOT copolymers, Macromol. Chem. Phys. 211 (2010) 1610–1617.

Figure legends

Figure 1. FT-IR spectra in KBr pellets of pure APG (1), APG functionalized with glutaraldehyde, APG-G (2), and SBP immobilized on APG, APG-G-SBP (3), compared with those of glutaraldehyde (G), and SBP.

Figure 2. SEM images of APG as such, APG-G and APG-G-SBP at two different magnification degrees.

Figure 3 Pore size distribution in each step of the SBP immobilization procedure as obtained via BJH model applied to desorption data: APG as such (△, dotted line), APG-G (□, dashed line), and APG-G-SBP (●, solid line).

Figure 4. ESR spectra at 4.7K of free and immobilized SBP (*g* values are reported near the spectral lines). The instrumental parameters were as follows: receiver gain, 10^5; modulation amplitude, 10 Gauss; modulation frequency, 100 KHz; power, 2 mW; time constant $8.192 \cdot 10^{-2}$ s; microwave frequency 9.44 GHz.

Figure 5. Effects of the initial amount of enzyme on the SBP load onto APG (●, solid line), and the yield of the immobilization process (○, dashed line).

Figure 6. Effect of pH on the specific activity towards guaiacol of immobilized, APG-G-SBP (●, solid line), and free SBP (○, dashed line). Experimental data were obtained in triple at 25 °C and fitted with a modified Henderson-Hasselbach equation.

Figure 7. Evaluation of the reaction product formation by APG-G-SBP in a little sized reactor: A) continuous process with DMAB-MBTH system at flow rate 2.5 mL min^{-1}; B) reaction cycles with guaiacol as substrate and 30 min of residence time in column.

Figure 8. Storage test of the immobilized enzyme stored at 3° C in dried form (●, solid line), and suspended in phosphate buffer 0.1 M pH 7.0 (■, dashed line), compared with free SBP conserved in the same solution (○, dotted line). Specific activities towards guaiacol were obtained in phosphate buffer pH 7.0 at 25 °C and reported as a percentage of the starting activity of each sample.

Table I: Main morphological aspects of APG as such, APG functionalized with glutaraldehyde and SBP immobilized on APG.

	APG	APG-G	APG-G-SBP
Particle size (μm)	55-100	20-80	20-80
Surface Area (m^2/g)	42	47	53
Mesopore volume (cm^3/g)	0.14	0.18	0.16
Average pore diameter (Å)	980	930	980

Figure 1

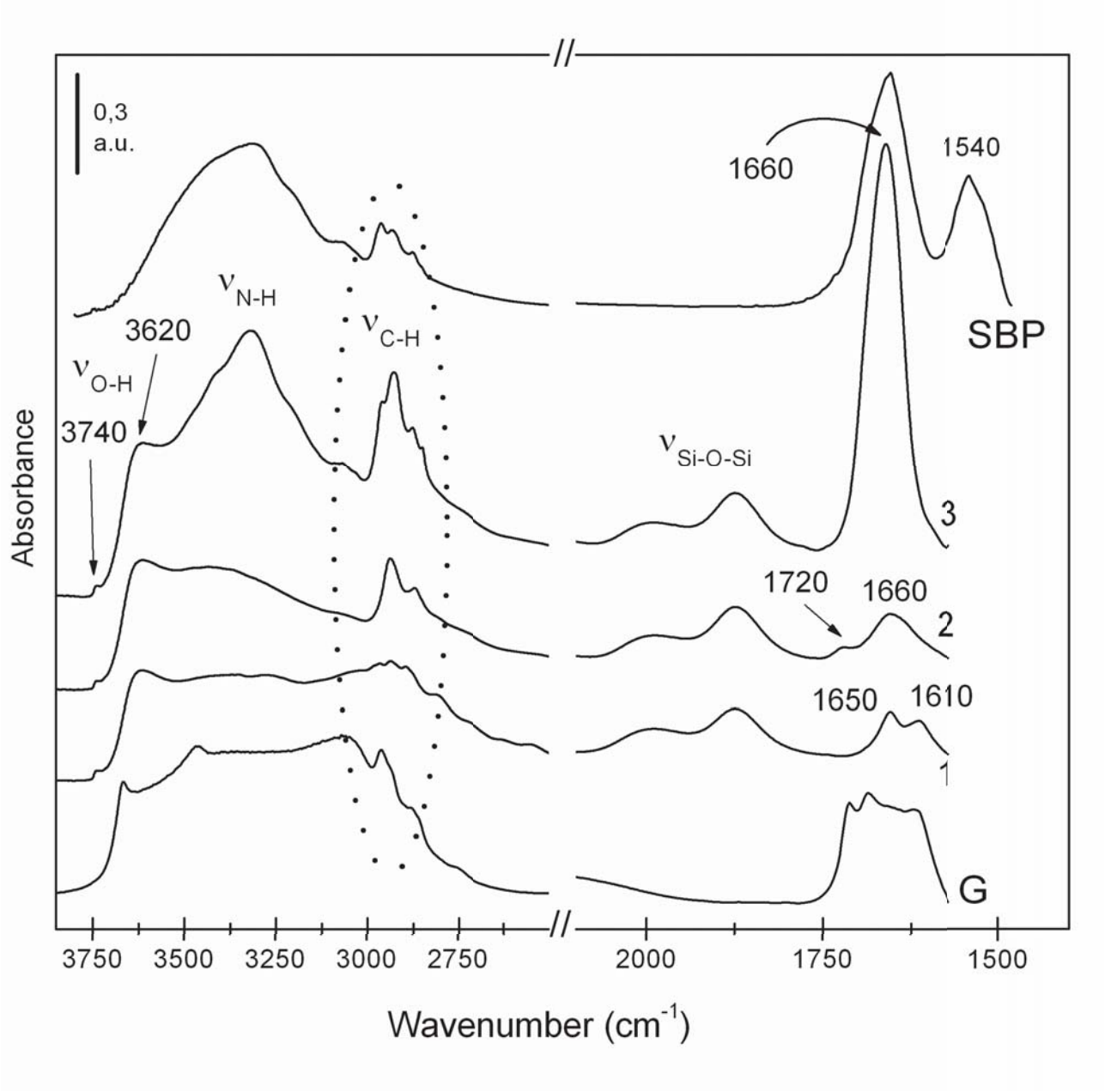
0,3
a.u.
1660
1540
SBP
ν_{N-H}
ν_{C-H}
3620
ν_{O-H}
3740
$\nu_{Si-O-Si}$
3
1720
1660
2
1650
1610
1
G
Absorbance
3750
3500
3250
3000
2750
2000
1750
1500
Wavenumber (cm^{-1})

Figure 2

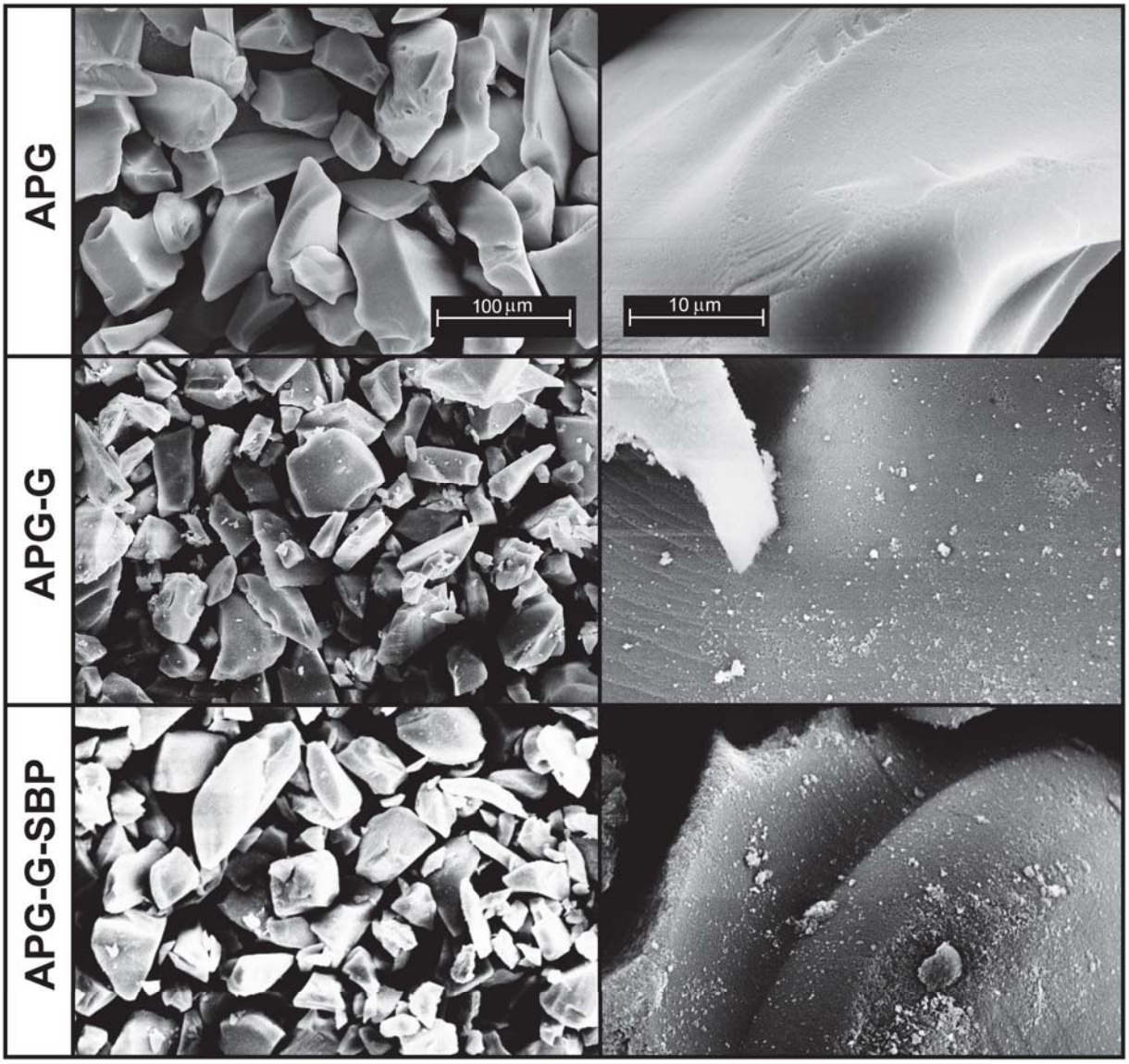

Figure 3

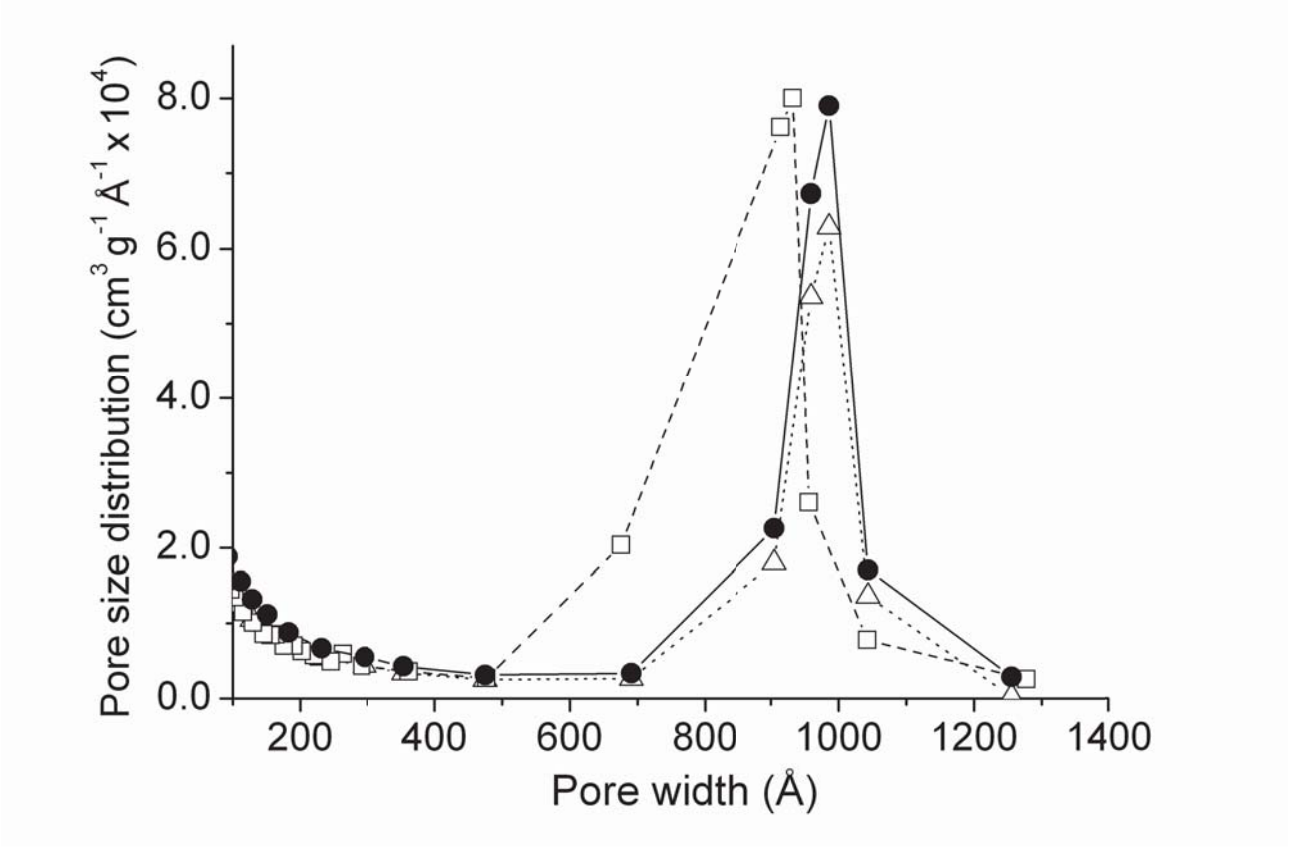
Pore size distribution (cm^3 g^{-1} Å^{-1} x 10^4)
8.0
6.0
4.0
2.0
0.0
200
400
600
800
1000
1200
1400
Pore width (Å)

Figure 4

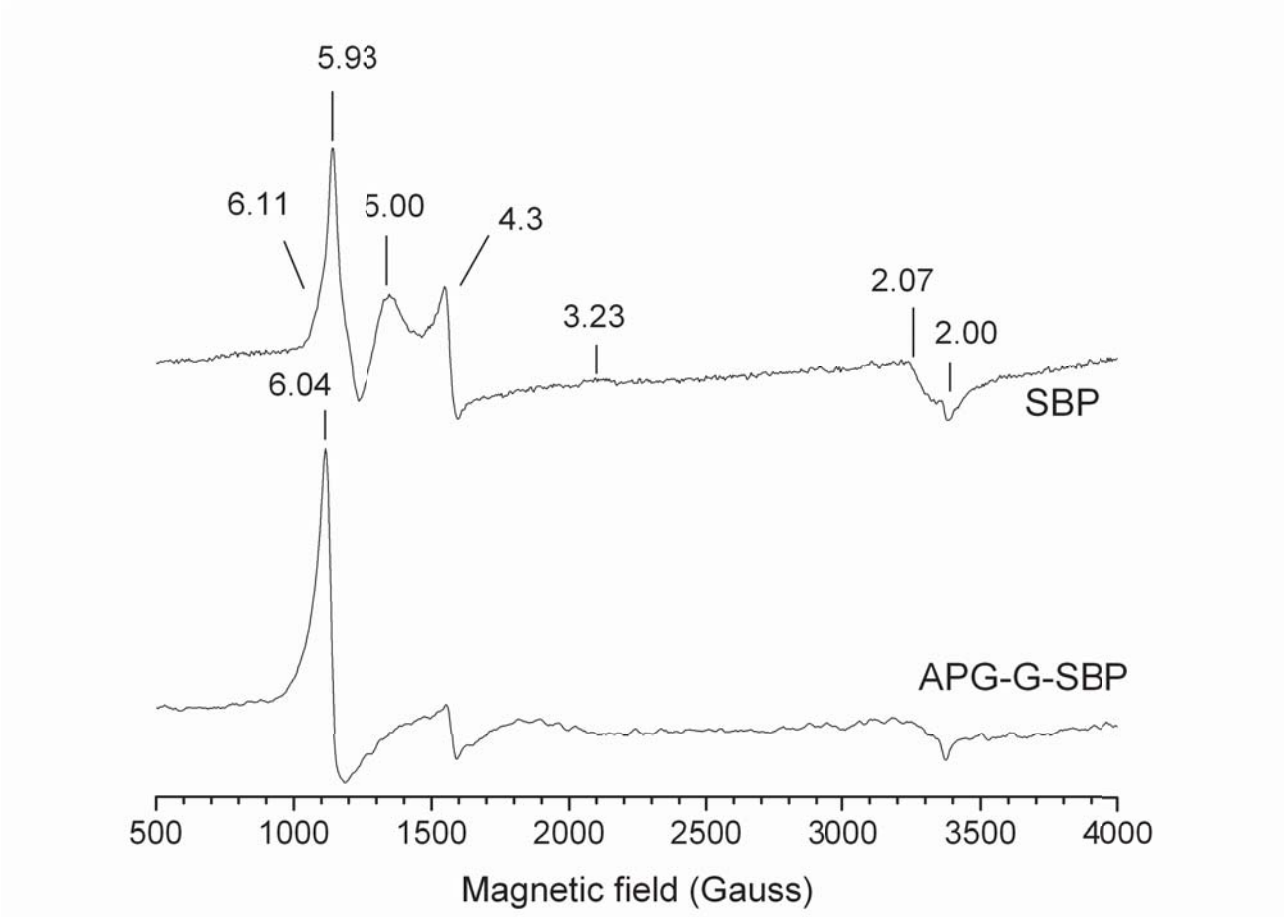
5.93
6.11
5.00
4.3
2.07
3.23
2.00
6.04
SBP
APG-G-SBP
500
1000
1500
2000
2500
3000
3500
4000
Magnetic field (Gauss)

Figure 5

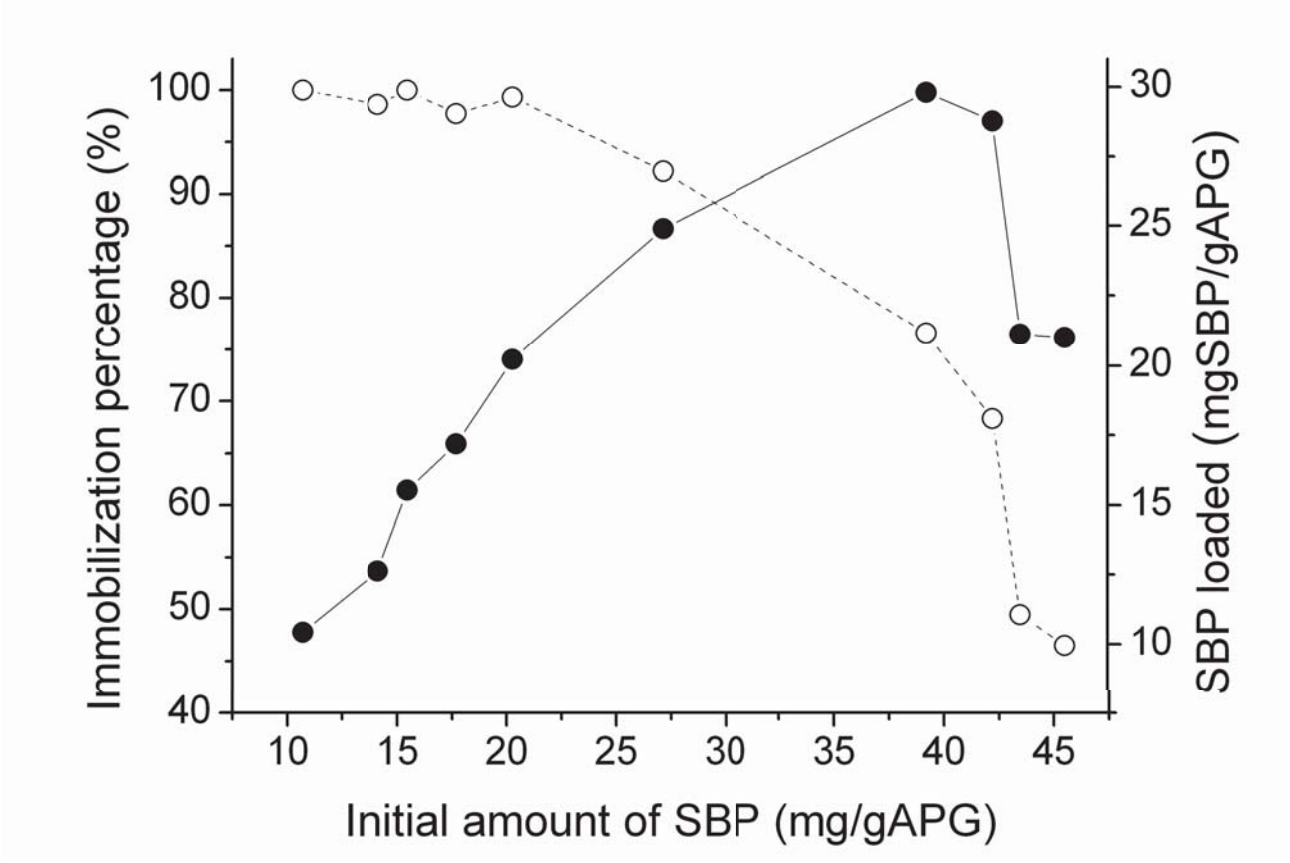
Immobilization percentage (%)
SBP loaded (mgSBP/gAPG)
Initial amount of SBP (mg/gAPG)
100
90
80
70
60
50
40
30
25
20
15
10
10
15
20
25
30
35
40
45

Figure 6

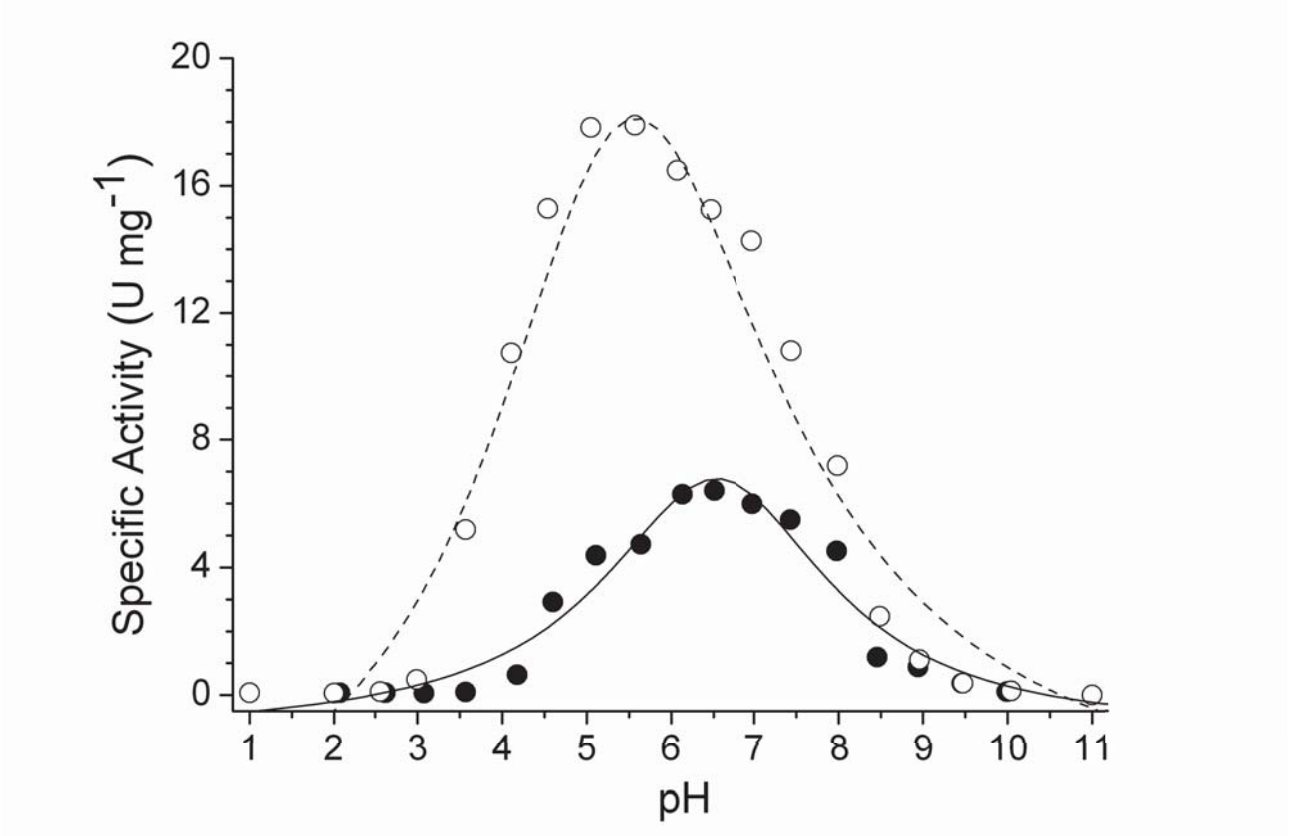

Figure 7

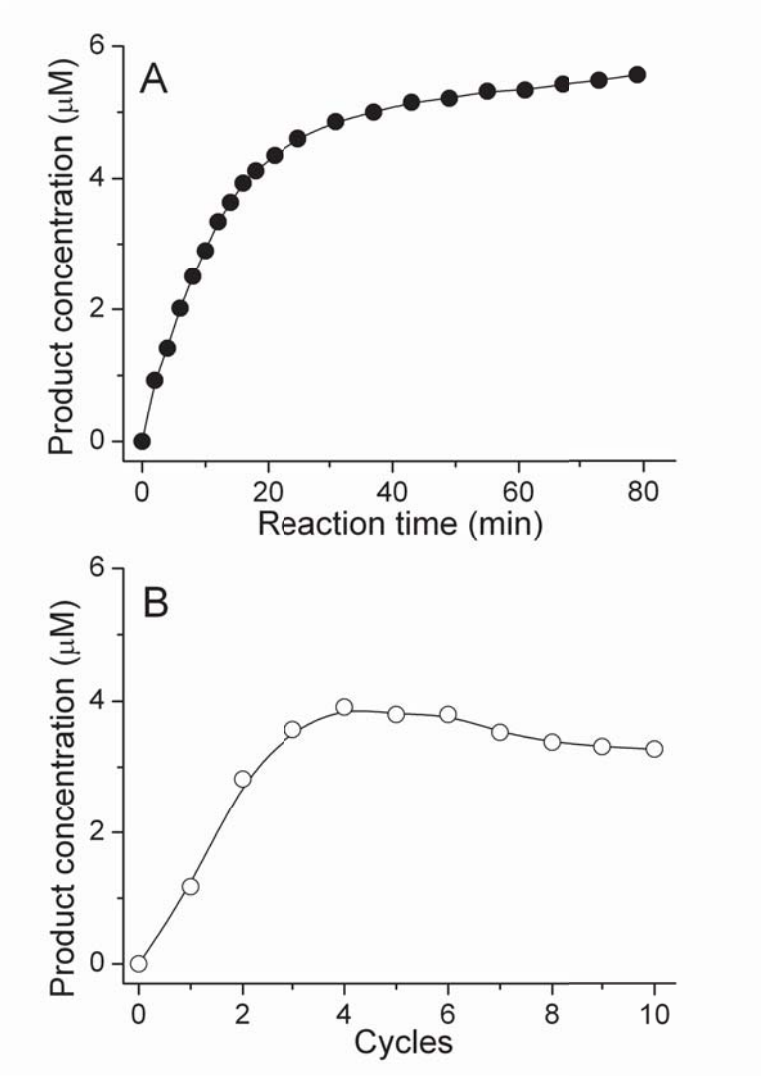
A
Product concentration (μM)
0
2
4
6
0
20
40
60
80
Reaction time (min)
B
Product concentration (μM)
0
2
4
6
0
2
4
6
8
10
Cycles

Figure 8